Chapter 9 - The Archaeological Application of the Data

The results presented so far have aimed to elucidate how bone density is influenced by a number of factors. Although this increases our understanding of bone density as a whole, it is of limited use in archaeological interpretation. In this chapter it will become apparent that, when interpreting archaeological sites, it is often not possible to ascertain the sex, breed or month of death of the material being studied. Consequently, data relating to these variables are of limited use. Instead, data relating to archaeologically visible variables (namely bone fusion) are of much more value when interpreting archaeological assemblages. Density data that are relevant to archaeological interpretation will be presented and their potential for predicting bias in element frequencies will be discussed. The potential implications of these data on archaeological age profiles will then be discussed. Next, this density data will be applied to the Neolithic site of Çatalhöyük in Turkey. First the site will be introduced. Then the data will be used to identify the impact of destructive taphonomic processes on its element frequencies. This part of the analysis will differ from those previously used (eg Kreutzer 1992, Lyman 1984, Elkin 1995 – see section 9.4.4). Instead of relying on the comparison of element frequencies and specific bone density values, this chapter will incorporate the density *ranges* identified in the previous chapter into the analysis. This will partly overcome the problem that the actual density of a bone cannot yet be reliably predicted, although the range of density values into which a scan-site is likely to fall has been more confidently determined. The precise processes responsible for any bias will be explored with reference to "taphonomic signatures" (eg gnaw marks, burning and fragmentation). Finally, the impact of these processes on the age profiles from the site will be explored and discussed.

9.1: The Presentation of Data Suitable for Use in Archaeological Interpretation

9.1.1: Introduction

The previous chapter shed some light on how and why bone density varies between the animals used in this project. This was enabled by the fact that certain details are known about the experimental material (in terms of the animals' age, sex,

breed etc.). When it comes to applying these data to an archaeological assemblage of sheep bones, the situation is different in that these details are unknown. Consequently, although we know that a certain degree of density variation exists between male and castrate sheep, this knowledge is of limited direct archaeological use, since it is often not possible to differentiate reliably between males and castrates in the archaeological material. It is therefore necessary to examine the variation within the experimental material as a whole, using categories that *could* be derived from an archaeological assemblage.

Also, the age of the animals examined by this project so far has been established to within approximately one or two days. Such a high resolution of ageing is not possible when examining archaeological material. Instead, when the data are used to interpret an archaeological faunal assemblage, only four age categories will be used. These are "neonatal", "unfused", "fusing" and "fused" and relate to the fusion status of whichever scan-site is under analysis. Centres of fusion do not occur in the midshaft region of bones. Fusion data are therefore not available for bone shafts and so, for these scan-sites, only two age categories can be used: neonatal and "post-neonatal". For the purposes of this project, neonatal bones will be defined as bones from animals that were a few days old or less at death. In practise this refers to animals numbers 6, 7, 11 and 17, which were zero (fetal), zero (fetal), zero (stillborn) and three days old at death, respectively. Although animal number 11 is known to be older than animals numbers 6 and 7, the extent of this age difference is unknown. Each of these four individuals is characterised by having bones (including their cortical bone) with a distinctive spongy appearance. "Post neonatal" bones are all of those from animals that do not fit these criteria. An epiphysis is said to be fusing when the epiphysial fusion line is clearly visible, but the epiphysis is attached to the diaphysis.

9.1.2: Presentation of the data

Box and whisker plots are very well suited to display the variability and distribution of the density data produced for each scan-site. The box and whisker plots used in this project show the range of density values obtained for each scan-site by means of a vertical line, or "whisker" (the upper and lower extremities of which correspond to the upper and lower extremes of the data). These plots also show the interquartile and median values of the data. The interquartile range represents the middle 50% of the ranked values and appears as a shaded rectangular area or "box". The median value is shown as a horizontal line across the interquartile range. The plots also

show values that are considered as being outliers (those that are greater than 1.5 box lengths from the upper or lower edge of the box). These are marked as "o". The skeleton number from which these data are derived is specified.

By examining box and whisker plots for the unfused, fusing and fused experimental material (and that from the shaft scan-sites), it will become apparent that the data follow a distinct trend. However, the data for the neonatal material are slightly more complex and require a little more explanation. For this reason, the post-neonatal material will be examined first, and then the slightly more complex discussion of the neonatal material will be undertaken.

9.1.3: Post neonatal animals – results and discussion

Figures 9.1 - 9.4 are the box and whisker plots for the post-neonatal material used in this project.

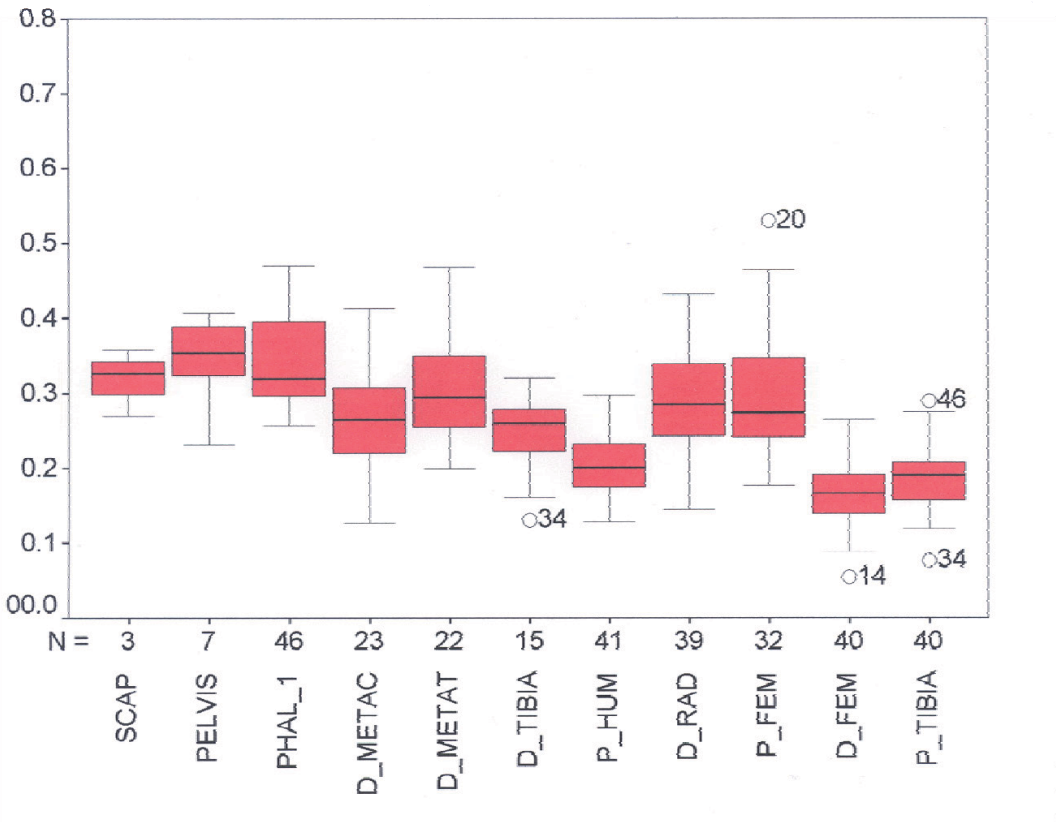

Figure 9.1: Showing the median, interquartile range, total range outliers and extreme density values of each scan-site. Only data from unfused elements are used. "N" is the number of observations possible for each scan-site.

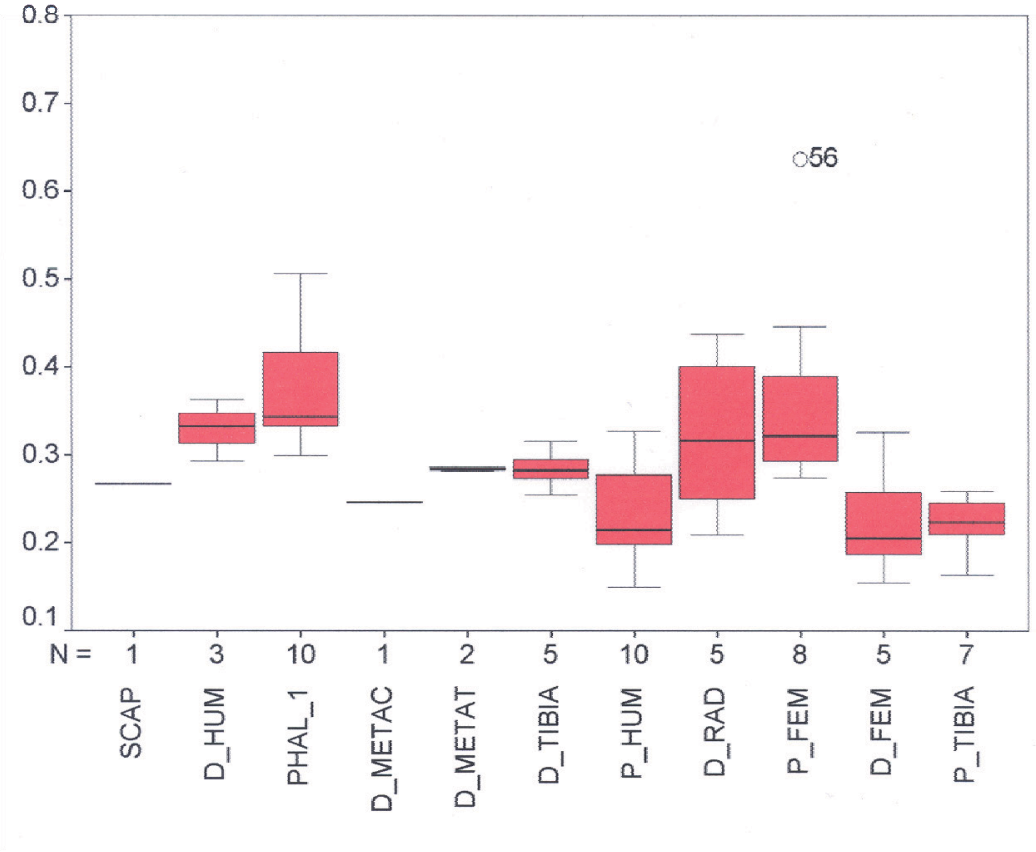

Figure 9.2: Showing the median, interquartile range, total range outliers and extreme density values of each scan-site. Only data from fusing elements are used. "N" is the number of observations possible for each scan-site.

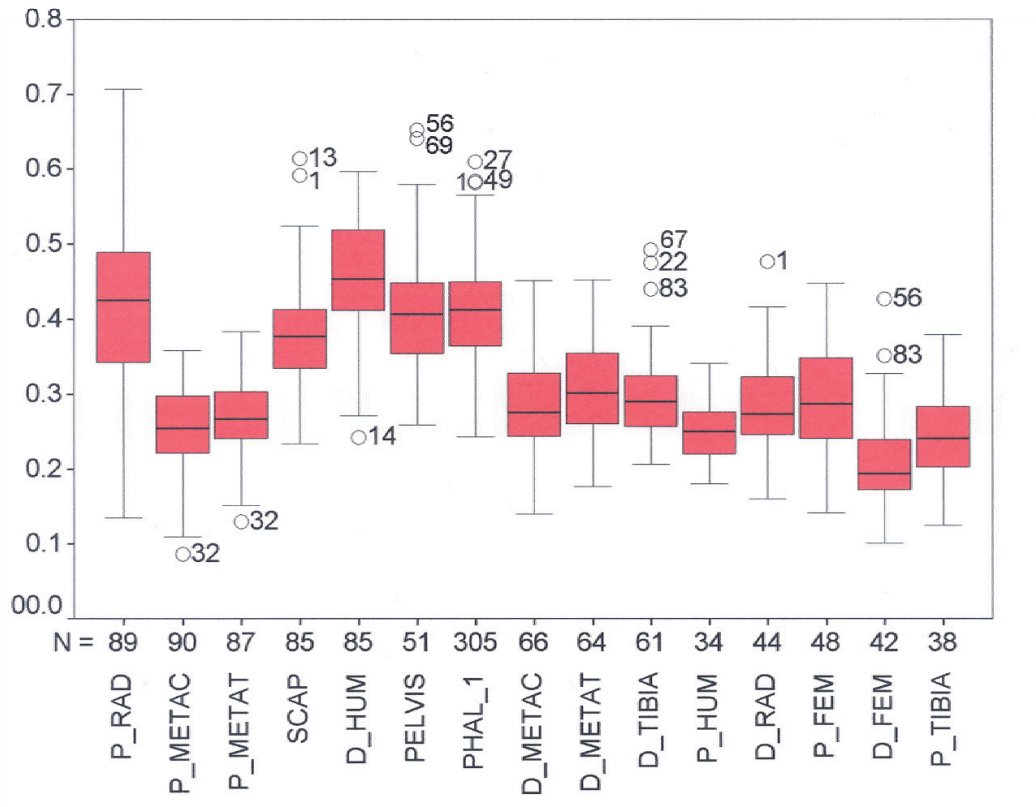

Figure 9.3: Showing the median, interquartile range, total range outliers and extreme density values of each scan-site. Only data from fused elements are used. "N" is the number of observations possible for each scan-site.

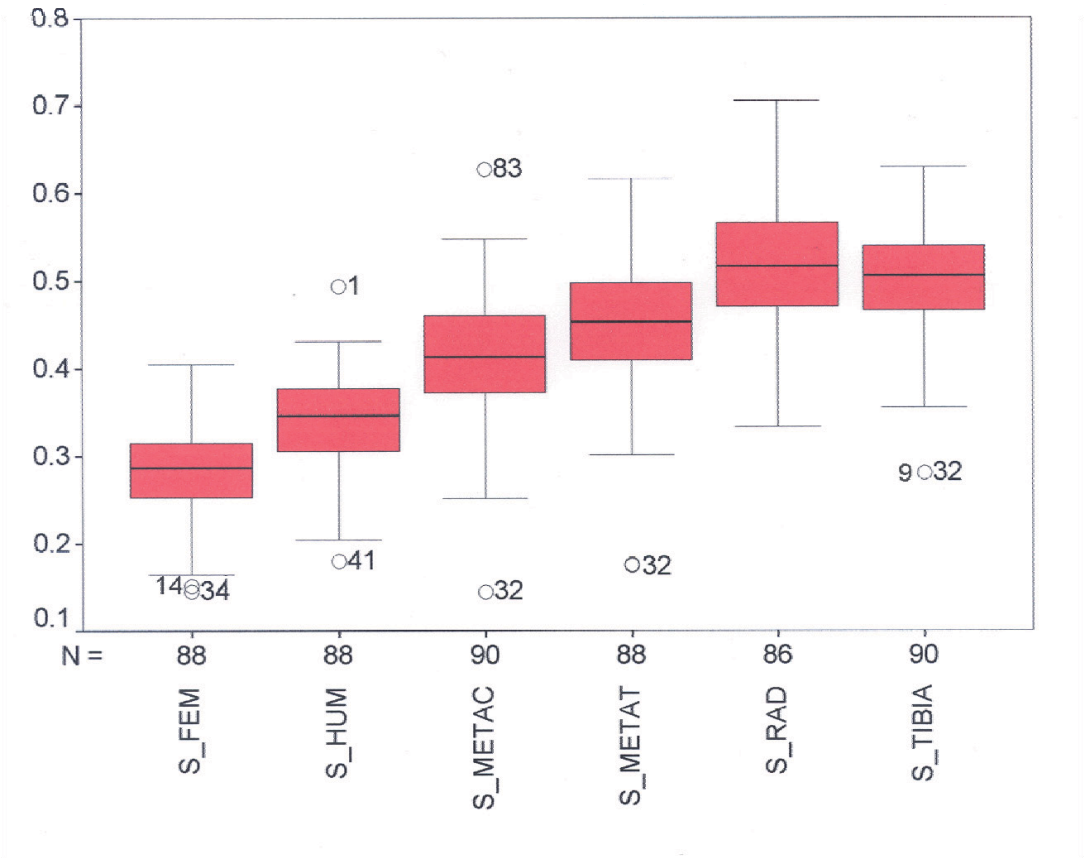

Figure 9.4: Showing the median, interquartile range, total range outliers and extreme density values of each scan-site. Only data from shafts are used. "N" is the number of observations possible for each scan-site.

Figures 9.1 - 9.4 are derived from the density data produced by this project. Although each age category is plotted separately, the material has not been subdivided in any other way. The data therefore relate to the bone density of animals of a variety of sexes, breeds, months of death etc. It is assumed that the ranges produced will therefore encompass the density values produced by animals of unknown origins (such as would normally be recovered archaeologically).

It should be noted that relatively few fusing elements were available for study and so the data relating to these elements are derived from a comparatively small sample. This explains why, in figure 9.2, the fusing distal metacarpal and scapula are represented by only a horizontal line: the sample size for each of these scan-sites was only one.

Each feature of figures 9.1 - 9.4 (the overall density ranges, interquartile ranges, median values and outliers) will be described and discussed in turn.

9.1.3.1: *Density range – "Whiskers"*

The "whiskers" in figures 9.1 - 9.4 show that the data for the post-neonatal material tend to fall into a comparatively wide range of values. This degree of variation in bone density values has also been observed (although not always commented on) by Lyman (1982), Ioannidou (2000) and Trotter and Hixon (1974). Broad data ranges such as these result in considerable overlap between the densities of different scan-sites. It is therefore not possible categorically to state that one scan-site will necessarily always be denser than another. It might be expected that unfused distal femora are less dense than unfused distal metacarpals. However, the relative densities of these two scan-sites could quite conceivably be reversed if a distal femur is a comparatively dense example and a distal metacarpal falls into the lower extreme of its density range. In some instances (eg the fused proximal humerus and the fused proximal metacarpal) the overlap is complete, in which case the density of one scan-site will always fall within the density range of another. Previous studies have often relied on ranking scan-sites in terms of their bone density (Brain 1976 p114, Butler and Chatters 1994 pp417 - 420, Elkin 1995 pp33 - 36, Kreutzer 1992 pp289 - 290, Lyman 1984 pp282 - 292 Willey *et al* 1997 p524). These analyses rely on specific density values for each scan-site under consideration. They work on the premise that where a faunal assemblage contains large numbers of high density body parts and relatively few low density body parts, the material has been subjected to some degree of taphonomic destruction. The comparison of body part frequencies and bone density values is most often achieved using Spearman's rank correlation coefficient (the higher the correlation coefficient, the more taphonomic destruction is assumed to have occurred).

Overlap in density ranges of any kind renders type of analysis problematic. It will often be impossible to predict, with any degree of certainty, whether an individual scan-site will be more or less dense (and so, prone to destruction) than another. The overlap in density values noted here is therefore likely to present considerable problems to any taphonomic analysis that employs the rank based methods that have previously been used.

An instance where the data range is especially broad is the fused proximal radius. This broad range of density values for the proximal radius is also evident in appendix D. The considerable variability in bone density values for this scan-site can be explained as a methodological artefact and requires some particular attention. Figure 9.5 is a pair of radiographs of two proximal radii. The position of the scan-site is marked on each.

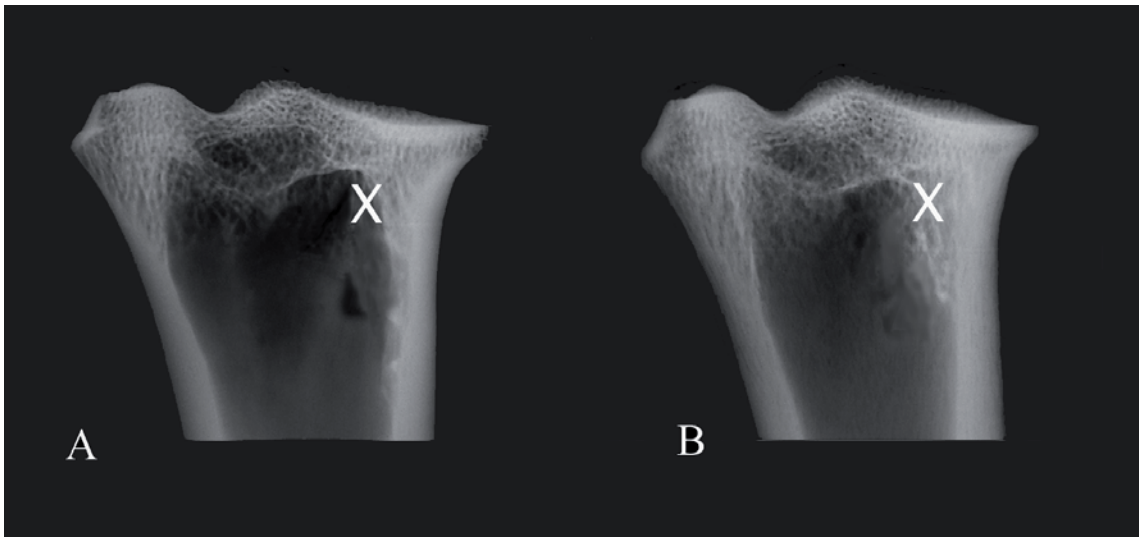

Figure 9.5: Showing two radii with very similar external morphologies. An "X" denotes the scan-site on each radiograph. It is clear that slight inconsistencies in the internal structure of the bones will lead to the bone density values returned being very different. This difference will not reflect either any differences in true density, or significantly different mechanical characteristics.

It is clear that the radiodensity of the scan-site of radius "A" will be considerably lower than that of radius "B", although the total thickness of the two bones will be comparable. This will result in "A" returning a lower bone density than "B". This is due to slight inconsistencies in the internal structure of this part of the radius rather than genuine variations in actual bone density. It is for this reason that data relating to the proximal radius must be deemed unsuitable for use in taphonomic analysis.

9.1.3.2: *Interquartile range – "Boxes"*

A partial solution to the problem caused by overlap in the overall density ranges can be afforded by the interquartile ranges displayed in figures 9.1 - 9.4. The fact that the interquartile ranges are small (compared with the overall ranges of each scan-site) indicates that the majority of the density values are clustered within a relatively small range. While it has already been noted that the unfused distal femur and distal metacarpal overlap in terms of their bone density, the interquartile ranges of these two scan-sites display no such overlap. Since the interquartile range denotes where the density values for a particular scan-site tend to cluster, the likelihood that any particular distal femur will be higher than any particular distal metacarpal is comparatively low.

The same cannot be said about, for example, the fused proximal tibia and humerus, because in this case, even the interquartiles overlap.

It is apparent, therefore, that although significant overlap in the density ranges for each scan-site exists, interquartile ranges can be used to remove or reduce this overlap. It is for this reason that interquartiles are potentially a valuable tool in taphonomic analysis.

9.1.3.3: *Median*

The median values for the scan-sites are also marked in figures 9.1 - 9.4. These relate to a single value, rather than ranges, and so are useful if the skeletal densities are to be ranked. The suitability of the rank based methods previously used in taphonomic analysis is debatable, especially when the broad density ranges that exist in the experimental material mean that the rank order of a group of scan-sites can potentially fluctuate markedly. However, where rank based methodologies are used, the median value is a much more suitable statistic than the mean (which is almost universally employed). The reason for this is that averages are susceptible to the effects of outliers, while median values are much less so. Consequently, median values reflect the true nature of the data, without being adversely affected by unusual or extreme values.

9.1.3.4: *Outliers*

A note on the outlying values would also be appropriate. Where outliers have been identified, they effectively increase the overall density range denoted by the "whisker" element of the plots. This effect is occasionally dramatic (eg the fusing proximal femur). These outlying values may be caused by either genuine extreme values in the data, or by measurement error. An examination of the skeleton numbers from which the outlying values originate shows that certain skeletons are repeatedly represented. For example, the density of animal number 56 appears to be unusually high on three occasions, while animal number 32 displays notably low density values five times. This suggests that, at least in cases such as these, the outliers represent the true density values of individuals with unusually robust or depleted skeletons, rather than measurement error.

9.1.4: Neonatal animals – results and discussion

Now that the behaviour of the data from the post-neonatal material has been described, it can be contrasted with that of the neonatal material. Figure 9.6 is the box

and whisker plot of the density data relating to these animals. Importantly, only four such individuals were available for analysis and so figure 9.6 is based on a small sample.

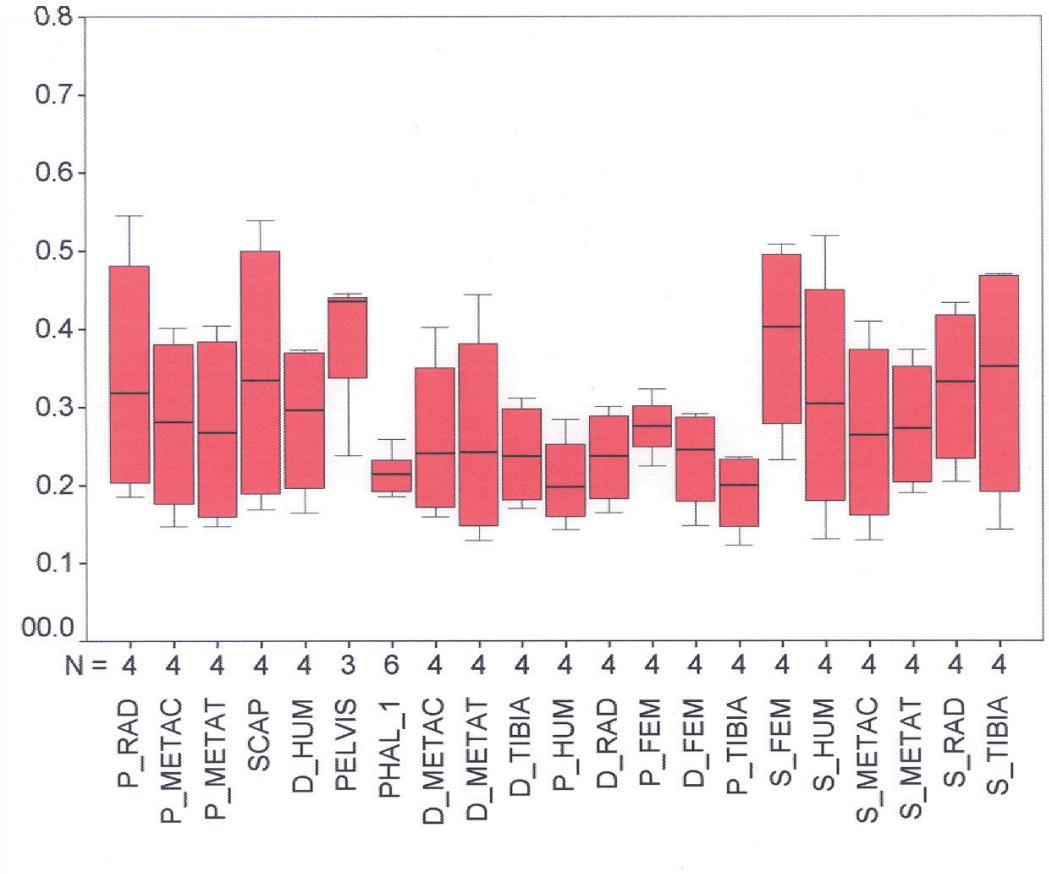

Figure 9.6: Showing the median, interquartile range, total range outliers and extreme density values of each scan-site. Only data from neonatal animals are used. "N" is the number of observations possible for each scan-site.

The overall appearance of figure 9.6 is quite different to that of the post-neonatal plots. For the majority of the scan-sites the interquartile ranges are large, and are frequently comparable to the overall range in their magnitude. This indicates that, unlike the post-neonatal data discussed above, the density values from this material do not tend to cluster around a single value.

The reason for this may lie in the small sample being used here. Such a small sample means that a single comparatively extreme value will have a disproportionately great effect on the interquartile range. However, a brief examination of figures 9.1 – 9.4 shows that where the sample size is small for the post-neonatal material (in the fusing distal humerus, for example), the broad spread of interquartile values observed for the

neonatal data does not exist. It cannot be categorically stated, therefore, that a small sample size will necessarily result in a broad range of density values being produced. Clearly an alternative explanation must be sought.

Perhaps such an explanation, is apparent in figure 8.3 (see section 8.2.1.2). This figure shows a sudden and rapid decrease in bone density around the time of birth. Although the ages of these animals are known to be different (see section 7.2.4), they all fall into the definition of "neonatal" used by this project. It is quite possible that, where this characteristic broad density range is seen, some of the material is from animals that had not experienced this drop in density, while the rest may have done. If this is the case, further research on a larger sample could be expected to produce a pattern of a wide range of densities, with an approximately equal number of examples in each density category. Alternatively the pattern produced might form two distinct peaks: one at the upper limit of the distribution and one at the lower. Only further research on a larger number of individuals will be able to determine which of these possibilities is the case.

9.1.5: Summary and some implications for the analysis of element frequencies from archaeological sites

- The bone density of a scan-site could appear anywhere within what is frequently a broad range of density values. This is contrary to the assumptions of previous taphonomic studies that have (wittingly or otherwise) tended to be based on fixed density values.
- Overlaps in the range of densities described above mean that it is frequently difficult to predict which scan-site will be denser than another. Consequently, predicting which scan-sites will tend to survive destructive taphonomic processes is equally difficult.
- The case is not so straightforward for neonatal individuals. Since neonatal material undergoes dramatic and sudden changes in its density, these bones have a potentially very wide range of density values. The result is that the overlap in density of these bones is considerable and reliably predicting which bones are likely to be more or less dense than others is not possible (even if such predictions are based on the interquartile ranges only).

The points raised by this chapter so far have fundamental implications for the way in which element frequencies within archaeological faunal assemblages are analysed. As mentioned previously, element frequencies can provide information about animal butchery and processing strategies in the past, including economic decisions and carcass transport. However, it has also been demonstrated that destructive taphonomic processes tend to remove lower density bones from an assemblage before affecting higher density bones. This has the potential effect of introducing bias into the element frequencies of an assemblage which, if not recognised and accounted for, might lead to misinterpretation of the data (see section 2.3).

The method most often used to assess the impact of destructive taphonomic processes on an assemblage relies on the comparison of fixed density values with element abundance. If this comparison reveals that the densest bones are also the most common, then taphonomic destruction is implicated as being (at least partially) responsible for the formation of the assemblage. Until the exact nature of the relationship between bone density and bone destruction has been established, it is impossible to account for taphonomic bias objectively. In the absence of such objective methods, the points below aim to offer general guidance as to how the methods previously used might be adapted and improved to take account of the findings of this chapter so far.

- Fixed density values are not a suitable tool for assessing the likelihood that a bone will be destroyed by taphonomic processes. Instead, a method that relies on the analysis of density *ranges* is preferable.
- It may be beneficial to concentrate on a small number of elements (or parts of elements) when assessing the extent to which an assemblage has been density mediated. Ideally these elements would be chosen because they have little or no overlap in their density ranges. Consequently, the elements being examined can confidently be ranked from least to most dense.
- Where it is impracticable to use elements that do not overlap in their density ranges (due to small sample sizes for example), overlap can be minimised by referring to the interquartile ranges of each scan-site's density.
- If an analytical method that requires fixed density values is to be used, median values may provide a more appropriate value than averages.

The following section will concentrate on the impact of the data produced by this project on the analysis of age profiles from archaeological sites.

9.2: The Implications of the Results for the Use of Age Data in Archaeological Interpretation

The above discussion focussed on how bone density values vary between and within specific scan-sites. This provides a fuller understanding of how bone density varies across the skeletons of similarly aged animals and enables a more appropriate use of bone density data for the analysis of element frequencies. It does not, however, significantly aid the interpretation of age profiles of archaeological material that has been subjected to destructive taphonomic processes. The following section will endeavour to highlight the differences in bone density between animals of different ages. The implications of these findings for the analysis of archaeological age profiles will then be discussed.

9.2.1: The comparative density of unfused, fusing and fused bones

The discussion in section 8.2.3 and 8.9.3 suggested that as an animal matures, its skeleton undergoes changes in density. This conclusion was based on the observation of material whose age at death was known to within one or two days. The age at death of archaeological material is seldom so clearly defined, and so data of such high resolution cannot be directly applied to archaeological investigations. This section will assess how the densities of the different age categories compare with one another. The categories to be examined here are based on bone's fusion stages. Bone fusion is an age related phenomenon that can be observed readily in the archaeological record. Combining the material into a small number of broad age categories will have the effect of significantly increasing the size of each.

So that an assessment of the variation in bone density between the age categories can be made, a further box and whisker plot was devised. This plot (figure 9.7) is derived from the same data as those discussed in the previous section. However, since the data for fusing material was based on a small sample and so was prone to erroneous results, it has been omitted from this analysis. It will later be seen that the behaviour of fusing bone in terms of bone density is somewhat unusual. The omission of these data at this stage is therefore justified. In addition, because the data from the neonatal material do not behave in the same way as those from older material, these data were also

excluded from this analysis. The behaviour of the neonatal data has been described and explained above and including it here will serve only to obscure any other patterns.

Figure 9.7 shows the density ranges of each of the scan-sites on unfused bones alongside the same information for each of the scan-sites of fused bones.

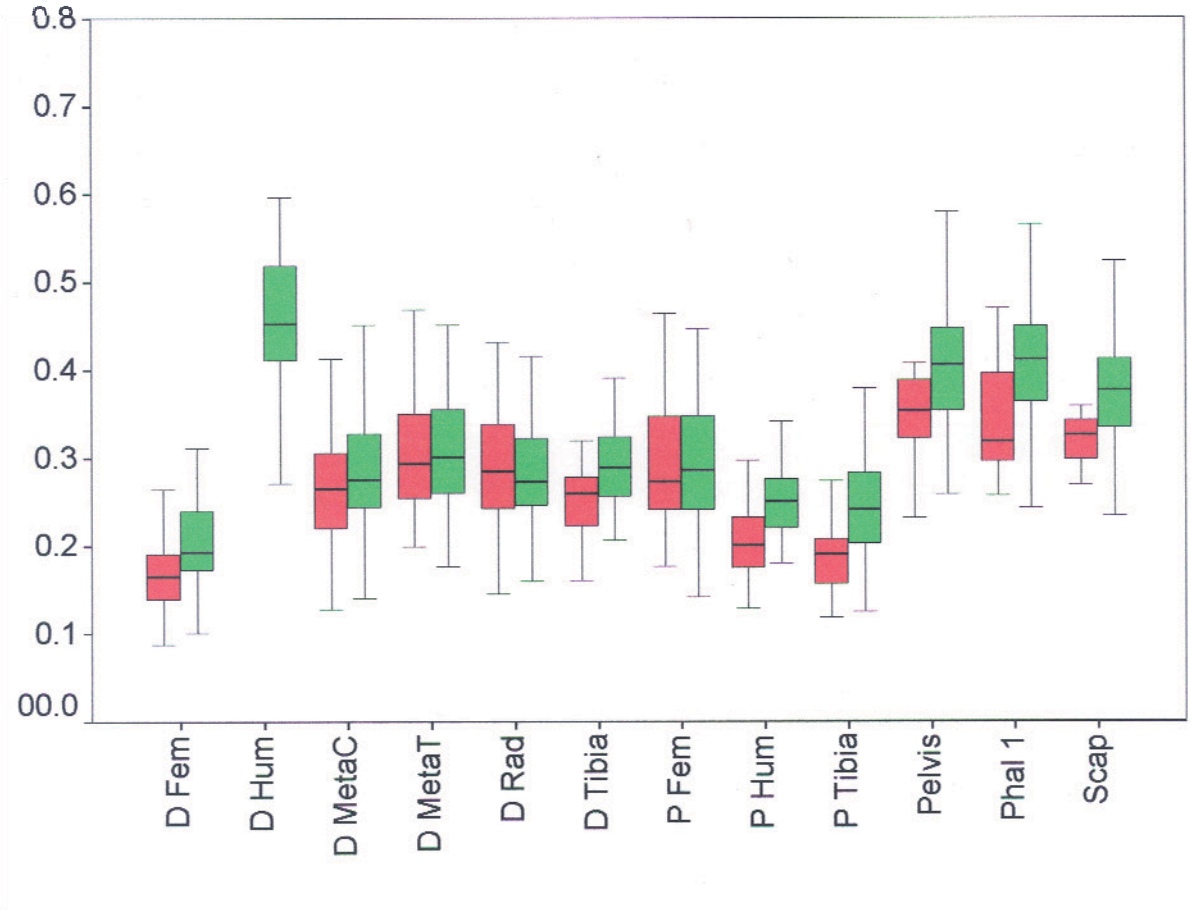

Figure 9.7: Showing the density ranges for the unfused (red) and the fused (green) material, so that the two can be compared.

9.2.1.1: *The tendency of unfused scan-sites to be less dense than fused scan-sites*

The overall trend apparent in figure 9.7 is rather a simple one. With only one exception (the distal radius) the unfused bone has a slightly lower density than the fused bone. This increase with age can be either slight (as in the distal metatarsal) or more marked (as in the proximal tibia). Compared with the inter-element variability, the differences between fused and unfused elements are slight.

9.2.1.2: *The tendency of certain bones to show a large discrepancy in density between fused and unfused specimens*

It is notable that the difference between the bone density of the fused and unfused material is not constant. This difference is greatest for the earliest fusing scan-sites (distal humerus, pelvis, first phalanx and scapula – all fused by 16 months). It is also considerable for many of the later fusing scan-sites (distal femur, proximal humerus and proximal tibia – all fusing between 3 and 3.5 years of age). The density difference between fused and unfused bone is comparatively slight for the scan-sites that fuse between about 1.5 and 3 years of age (eg distal metacarpal and metatarsal, distal radius and proximal femur). The implications of this observation for archaeological research will be discussed later.

With the exception of the neonatal material (which has been omitted from this analysis), no examples of unfused distal humeri were available to this project. It is therefore not possible to reach any conclusions regarding the relative densities of this scan-site in different states of fusion. However, it is worth noting that a comparison of the *fusing* and fused distal humerus showed the former to be, overall, considerably less dense than the latter. This pattern is comparable with what was observed for other early fusing scan-sites.

9.2.1.3: *The tendency of the earliest fusing scan-sites to have the highest bone density*

Within this overall trend there are further observations that can be made. For example, the scan-sites with the highest densities are those that fuse at the earliest age (distal humerus, pelvis, first phalanx and scapula – all fused by 16 months), while the lowest density scan-sites are those that fuse latest (distal femur, proximal humerus and proximal tibia).

Furthermore, although a fused scan-site will tend to be denser than its unfused counterpart, *all* fused scan-sites are not necessarily denser than *all other* unfused scan-sites. For example, the unfused pelves are generally denser than the fused proximal tibiae.

9.2.2: Discussion of the age related variation of bone density

9.2.2.1: *The tendency of unfused scan-sites to be less dense than fused scan-sites*

It has long been assumed that immature (unfused) bone is less dense than mature (fused) bone and so is less likely to survive destructive taphonomic processes. The data

presented here support this. This analysis has demonstrated that there is a perceptible increase in bone density between categories of increasing age.

It is interesting that this analysis has not detected the decrease in bone density of older animals (perhaps associated with osteoporosis) that was noted in section 8.9.3. This could be because the "fused" category in this context incorporates animals that come from the full range of sexes and adult ages. If this density reduction is associated only with females or animals of considerable age (as would be expected), it is quite possible that slightly younger individuals or males and castrates are having the effect of masking this reduction in bone density.

The reasons for the increase of density with age are probably numerous. Maturing bone has been shown to increase in its calcium content and material density (the density of the bone material itself – excluding the effect of pores and cavities). It has also been shown to decrease in its porosity. Each of these three changes will cause higher bone density values to be returned by the methods used in this project. Moreover, each of these changes has been shown to result in reduced bone strength (Currey 1979b pp459 - 469).

9.2.2.2: *The tendency of early fusing bones to show a large discrepancy in density between fused and unfused specimens*

It was noted above that the difference in bone density between fused and unfused specimens is not constant and that for some scan-sites this difference is greater than for others. Of the scan-sites that exhibit this feature, some are notable in that they fuse very early in life (scapula, proximal first phalanx, pelvis and distal tibia and humerus). A function of this early fusion is that any unfused specimens will necessarily be very young. Table 9.1 compares the average ages of all of the unfused and fused specimens described in figure 9.7. The table also presents the ratio of the average ages of the fused and unfused material. This ratio shows, for example, that the fused pelves examined in figure 9.7 were, on average, 6.1 times older than the unfused pelves. Furthermore, the fused distal femora were, on average, only 4.0 times older than the unfused distal femora. This difference is reflected in the fact that the earliest fusing scan-sites show a greater discrepancy in bone density between fused and unfused specimens.

	Fusion Age in Months (From Silver 1969)	Average Age (in Months) of Unfused Material	Average Age (in Months) of Fused Material	Ratio of Average Ages
Scapula	6 - 8	3.8	56.1	15.0
Pelvis	6 - 10	8.8	53.4	6.1
Proximal First Phalanx	13 - 16	9.9	61.2	6.2
Distal Tibia	18 - 24	10.3	67.2	6.5
Distal Metacarpal	18 - 24	14.0	67.8	4.8
Distal Metatarsal	20 - 28	14.2	68.7	4.8
Proximal Femur	30 - 36	18.2	78.3	4.3
Distal Radius	36	20.1	82.2	4.1
Proximal Humerus	36 - 42	21.5	92.0	4.3
Proximal Tibia	36 - 42	21.3	87.4	4.1
Distal Femur	36 - 42	21.1	84.1	4.0

Table 9.1: showing the average ages of the fused and unfused examples of the scan-sites described in figure 9.7. The ratio of these average ages is also given. The ratio of the average ages for the scapula is particularly high because only three examples of unfused scapula were available for study and all were particularly young.

It is therefore possible to conclude that the large density difference between fused and unfused examples of early fusing scan-sites is a function of the *relative age* of the material concerned. In other words, bone density is mediated by an animal's age, rather than the fusion status of its bones, while the fusion status is merely an indicator of its age.

9.2.2.3: *The tendency of other, later fusing bones to show a large discrepancy in density between fused and unfused specimens*

Other, later fusing scan-sites (the proximal tibia and humerus, and distal tibia and femur) also show a relatively large density difference between fused and unfused specimens.

In order to explore this feature, it is first necessary to propose a model by which the bone density values develop throughout the life of an animal. Of these scan-sites, three (all except the distal tibia) consist of a relatively large articular surface. Where an articular surface is large, any stress transmitted through that articular surface will be absorbed by a relatively large volume of bone. Consequently, the shock absorbing properties (including the bone density) need not be as great as for other, smaller, articulations. This explains why the distal femur, proximal humerus and proximal tibia all have overall lower densities than other scan-sites. Scan-sites with smaller articular surfaces (eg the distal metapodia) need to be stronger in order to withstand more

concentrated impact stresses. As a result of this, it can be expected that these scan-sites are not only denser overall, but also reach this higher level of density quite early in life (in order to meet the structural requirements of the joint as quickly as possible).

The model being proposed is therefore one in which scan-sites associated with a large articular surface reach their maximum density gradually and relatively late in life, even though this density is comparatively low. Conversely, scan-sites associated with a smaller articular surface area have a higher density that is achieved earlier in life. This means that the difference in the densities of the two groups of bones will be greater in early life than in later life.

Figure 9.8 shows how the bone density of the scan-sites under discussion here changes throughout the life of an animal. The development of bone density for the small articular surfaces is contrasted with that of the larger articular surfaces. Figure 9.8 has been produced in the same way as figure 8.3 (ie by plotting the bone density of a number of arbitrarily selected animals arranged in order of increasing age).

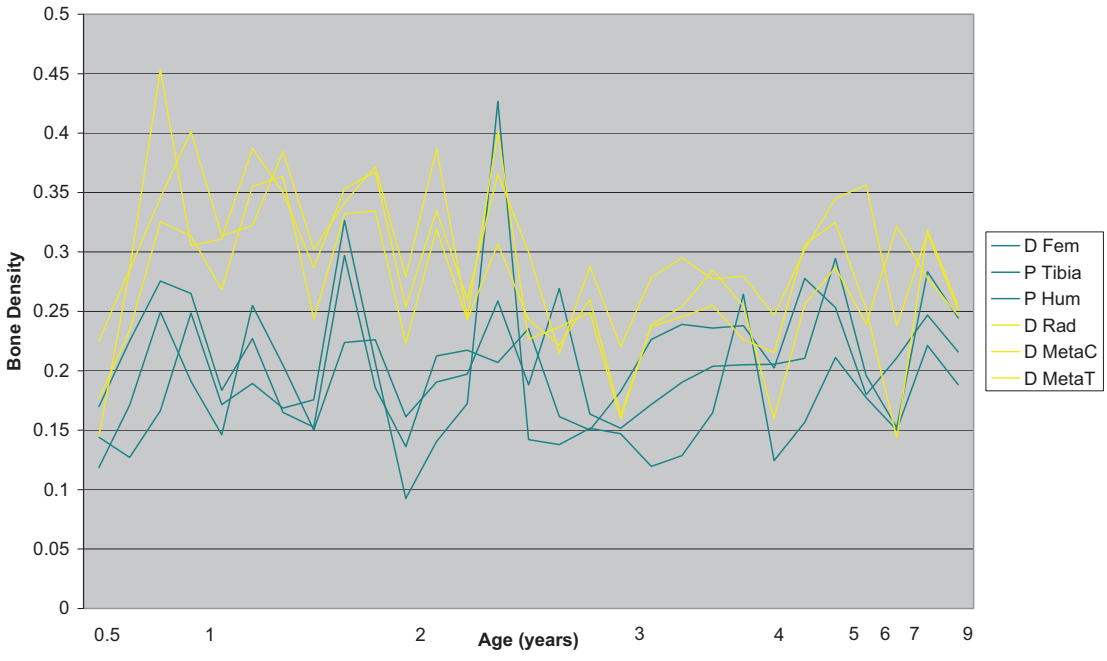

Figure 9.8: Contrasting the development of bone density of large and small articulations. The graph was produced by plotting the bone density of a number of different animals arranged in order of increasing age. Note that the increasing age along the x-axis is irregular. Green lines indicate large articulations, while yellow lines indicate small articulations.

The picture that emerges from figure 9.8 is confused by the considerable degree of background variation. However, it is possible to note that the large articulations are much less dense than the small articulations in early life (especially between one and two years of age) and the densities of the two groups of bones converge later in life (around five and a half years of age). This observation is in agreement with the predictions of the model proposed above.

It is now possible to use this model to explain why the larger articular surfaces exhibit greater density differences between the fused and unfused examples that the smaller articular surfaces. The model presented above suggests that the bone density of small articulations reaches its maximum relatively rapidly and then levels off. Consequently, the bone density before and after fusion will be quite similar. Since large articulations reach their maximum density more gradually, the density of an unfused specimen will be notably lower than that of a fused specimen. This can be demonstrated using hypothetical data, in figure 9.9 and table 9.2.

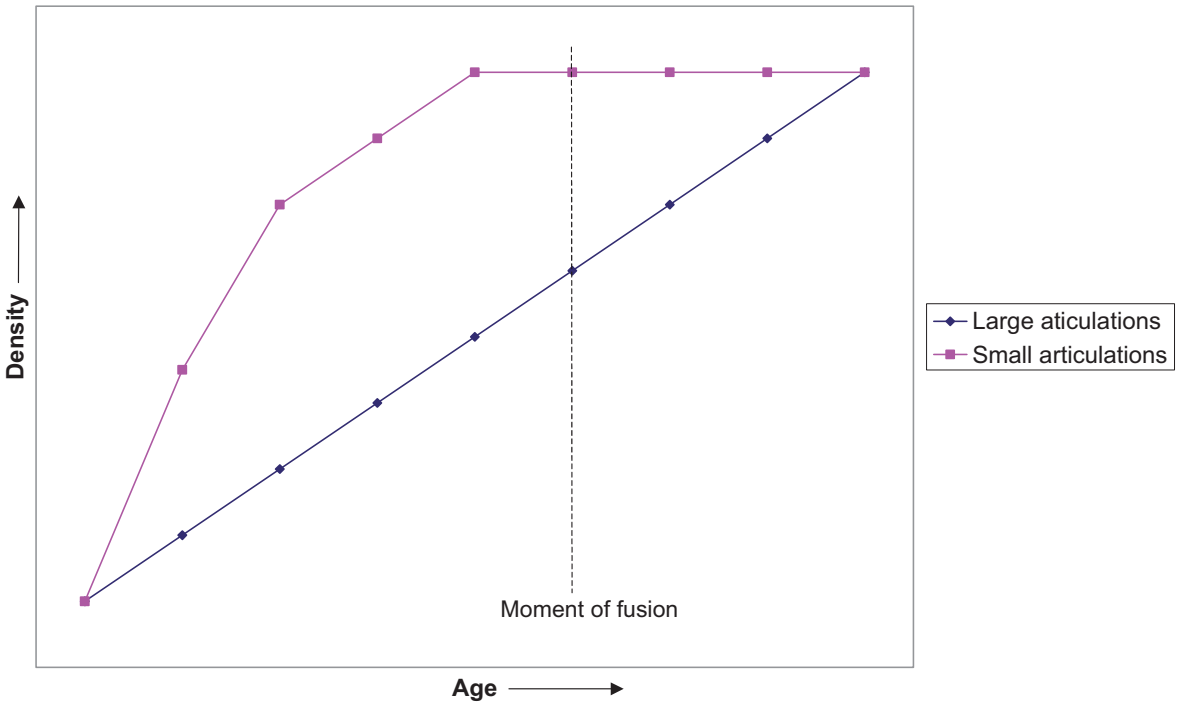

Figure 9.9: Showing a hypothetical example of the different development of the bone density of a large and a small articulation. Note that the small articulation reaches its maximum earlier in life. The moment at which the bones might fuse is also marked on the figure.

Increasing Age	Density of Large Articulation	Density of Small Articulation	Average Density of Large articulation (Before Fusion)	Average Density of Small Articulation (Before Fusion)
	1	1	3	5.9
	2	4.5		
	3	7		
	4	8		
	Moment of fusion		Average density (Fused)	Average density (Fused)
	5	9	7.5	9
	6	9		
	7	9		
	8	9		
	9	9		

Table 9.2: Showing the hypothetical density data from which figure 9.9 was produced. The moment at which the bones fuse is marked on the table. The average density values are intended to represent the average density of either fused or unfused material. Note that the difference between the fused and unfused large articulation is greater (4.5) than the same difference for smaller articulations (3.1).

Figure 9.9, table 9.2 and the discussion above have demonstrated that the difference in density between fused and unfused scan-sites can be related to the bone development. This bone development is, in turn, related to the functional anatomy of an animal. The arguments presented above have referred to the size of the articular surfaces concerned. It would be reasonable to argue that the density differences between fused and unfused material are instead related to skeletal location. This is because three out of the four scan-sites that exhibit a large density difference between fused and unfused specimens are from the hind limb. It is therefore arguable that it is hind limb scan-sites, rather than large articular surfaces, that reach their maximum bone density gradually, resulting in the patterns described above. It is also conceivable that the observed patterns are a combination of both of these two factors.

It would be prudent to note that the discussion presented here is conjectural and, until it has been backed up with more experimental data, cannot reasonably be accepted as the definitive interpretation of the data produced by this project.

9.2.2.4: *The tendency of the earliest fusing scan-sites to have the highest bone density*

The final point to be noted in figure 9.7 is that the highest density scan-sites are also those that are the first to fuse (the scapula, proximal first phalanx, pelvis and distal humerus). The reason for this may also be connected with the functional anatomy of the animals concerned. The high bone density of these scan-sites suggests that these parts of the animals are subject to greater levels of physical stress during life. As such, the high

density levels can be seen as an adaptation to these stresses. The early fusion of these scan-sites can also be seen as an adaptation to these stresses (since the parts of the skeleton required to be most robust are likely to be required to reach their mature state as early as possible). Again, this argument is somewhat conjectural. Further experimental research is required for verification.

9.2.3: The creation of age profiles from fusion data

Now that the nature of the density differences between unfused and fused material has been described and discussed, their effects on fusion derived age profiles require further attention. First, it is necessary briefly to describe the methods used to convert archaeological fusion data into an age profile.

Both dental methods and epiphyseal fusion methods are commonly used in archaeological analysis to create cull patterns that suggest a sequence of kill-off of animals within a notional population. This project will focus on the use of bone fusion data, since, although not without its drawbacks (Chaplin 1971 p81) the method is frequently used by zooarchaeologists who often have large samples of skeletal elements from which fusion data can be gleaned.

The method used to transform fusion data into age profiles for the archaeological material is outlined by Chaplin (1971 p128). This involves the creation of fusion categories consisting of groups of bone parts that fuse at approximately the same age. The percentage of unfused bones from each group can then be calculated. This figure relates to the proportion of animals that died (or were killed) before reaching the fusion age associated with that category. Although this basic method has been variously adapted, it retains a number of methodological problems (O'Connor 2000 pp92-96, Watson 1978). Such methodological problems include variation in skeletal maturation between distinct populations or according to sex or nutritional status (Moran and O'Connor 1994 pp273 - 275). However, methods based on epiphyseal fusion have the considerable advantage that data from the entire skeleton can be incorporated into the age profiles being produced. Different authors have devised a variety of different fusion groups. The groups to be adopted in this discussion will be those used by Halstead (1992 p36) and based on Silver (1969). They are shown in table 9.3.

Group Name	Fusion Time	Elements
Group 1	<6 months	Metacarpal III & IV Metatarsal III &IV
Group 2	6-10 months	Scapula Distal Humerus Pelvis First Phalanx
Group 3	18-28 months	Distal Metacarpal Distal Metatarsal Distal Tibia
Group 4	30-42 months	Proximal Humerus Distal Radius Proximal Femur Distal Femur Proximal Tibia

Table 9.4: showing the four fusion groups used in this project, their fusion times and the elements that comprise them. (After Halstead 1992 p36, table 3).

Figure 9.10 is a version of figure 9.7 in which the fusion groups described in table 9.4 are labelled. It is intended that figure 9.10 will complement the discussions that follow.

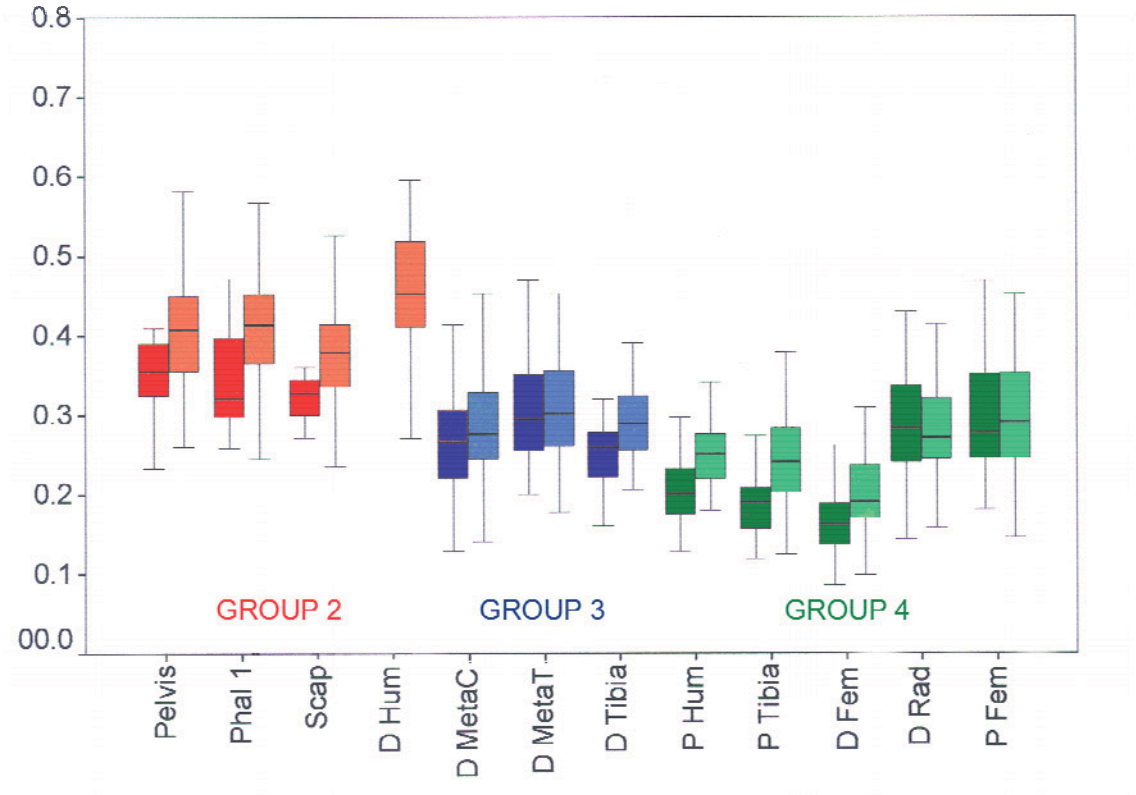

Figure 9.10: A simplified version of figure 9.7, intended to complement the following discussions. The paler colours relate to the fused material from each group.